Redox Biology 2 (2014) 436–446

Contents lists available at ScienceDirect

Redox Biology

journal homepage: www.elsevier.com/locate/redox

Identification of DUOX1-dependent redox signaling through protein *S*-glutathionylation in airway epithelial cells ☆

Milena Hristova [a], Carmen Veith [a], Aida Habibovic [a], Ying-Wai Lam [b], Bin Deng [b], Miklos Geiszt [c], Yvonne M.W. Janssen-Heininger [a], Albert van der Vliet [a,*]

[a] Department of Pathology, Vermont Lung Center, College of Medicine, University of Vermont, Burlington, VT 05405, United States
[b] Department of Biology, College of Arts and Sciences, University of Vermont, Burlington, VT 05405, United States
[c] Department of Physiology, Faculty of Medicine, and "Lendulet" Peroxidase Enzyme Research Group, Semmelweis University, Budapest, Hungary

ARTICLE INFO

Article history:
Received 16 December 2013
Received in revised form
23 December 2013
Accepted 23 December 2013
Available online 15 January 2014

Keywords:
DUOX1
NADPH oxidase
Cell migration
Cysteine
S-glutathionylation
Proteomics

ABSTRACT

The NADPH oxidase homolog dual oxidase 1 (DUOX1) plays an important role in innate airway epithelial responses to infection or injury, but the precise molecular mechanisms are incompletely understood and the cellular redox-sensitive targets for DUOX1-derived H_2O_2 have not been identified. The aim of the present study was to survey the involvement of DUOX1 in cellular redox signaling by protein *S*-glutathionylation, a major mode of reversible redox signaling. Using human airway epithelial H292 cells and stable transfection with DUOX1-targeted shRNA as well as primary tracheal epithelial cells from either wild-type or DUOX1-deficient mice, DUOX1 was found to be critical in ATP-stimulated transient production of H_2O_2 and increased protein *S*-glutathionylation. Using cell pre-labeling with biotin-tagged GSH and analysis of avidin-purified proteins by global proteomics, 61 *S*-glutathionylated proteins were identified in ATP-stimulated cells compared to 19 in untreated cells. Based on a previously established role of DUOX1 in cell migration, various redox-sensitive proteins with established roles in cytoskeletal dynamics and/or cell migration were evaluated for *S*-glutathionylation, indicating a critical role for DUOX1 in ATP-stimulated *S*-glutathionylation of β-actin, peroxiredoxin 1, the non-receptor tyrosine kinase Src, and MAPK phosphatase 1. Overall, our studies demonstrate the importance of DUOX1 in epithelial redox signaling through reversible *S*-glutathionylation of a range of proteins, including proteins involved in cytoskeletal regulation and MAPK signaling pathways involved in cell migration.

Introduction

The respiratory epithelium forms a first line of pulmonary defense against inhaled microorganisms, allergens and other pollutants, by creating tightly controlled physical barrier that minimizes microbial invasion and exposure of critical lung constituents to noxious environmental agents, and by evoking innate responses to diverse pathogen- or damage-associated molecular patterns to initiate host defense mechanisms and/or wound responses to infection or injury. One aspect of such innate responses is the apical production of hydrogen peroxide (H_2O_2) in response to various stimuli, originating primarily from two recently identified NADPH oxidase homologs, the dual oxidases 1 and 2 (DUOX1/2). This regulated H_2O_2 production is believed to represent an important component of oxidative antimicrobial surveillance at mucosal surfaces [1–4], although the relative roles of DUOX1 or DUOX2 in such mucosal host defense are still somewhat unclear [5]. In addition to its proposed involvement in apical oxidative host defense, epithelial DUOX reportedly also participates in autocrine or paracrine cell signaling mechanisms that regulate cellular pro-inflammatory and wound responses [6–9]. As such, DUOX has been demonstrated to control the activation of Src family kinases and epidermal growth factor receptors (EGFR), resulting in downstream cell signaling via extracellular signal-regulated kinase (ERK) and/or nuclear factor (NF)-κB [5,10].

Activation of DUOX in response to epithelial infection or injury often involves the initial secretion of cellular damage signals such as ATP, which promotes Ca^{2+}-dependent DUOX activation by

* Correspondence to: Department of Pathology, University of Vermont, D205 Given Medical Building, 89 Beaumont Avenue, Burlington, VT 05405, United States. Tel.: +1 802 656 8638; fax: +1 802 656 8892.
E-mail address: albert.van-der-vliet@uvm.edu (A. van der Vliet).

2213-2317/$ - see front matter © 2014 The Authors. Published by Elsevier B.V. This is an open access article under the CC BY-NC-ND license (http://creativecommons.org/licenses/by-nc-nd/3.0/).

http://dx.doi.org/10.1016/j.redox.2013.12.030

stimulation of purinergic P2Y receptors on the epithelial surface [10]. Within the respiratory tract, such ATP-dependent wound responses primarily rely on the major constitutive airway epithelial isoform, DUOX1, and our recent studies have demonstrated a key role for DUOX1 in ATP-dependent epithelial wound responses and epithelial regeneration [9,11,12], analogous to observed DUOX-dependent injury responses in zebrafish or Drosophila [6,8]. Nevertheless, in spite of reports indicating DUOX-dependent cell signaling through oxidation of selective cysteines within e.g. Src family kinases [8,11] or ADAM-family sheddases [11,13,14], no studies exist that systematically evaluate the cellular targets that are subject to redox-dependent regulation by activation of DUOX1. Moreover, while some studies suggest that DUOX1-mediated signaling involves selective oxidation of redox-sensitive targets in e.g. signalsomes (e.g. [11,15]), others imply that DUOX activation generates H_2O_2 gradients capable of paracrine oxidative signaling over several cell distances [7,16].

One important mode of oxidant-dependent redox signaling involves the reversible oxidation of selected protein cysteine residues, and one major consequence of such cysteine oxidation is the formation of a mixed disulfide with GSH, the most abundant cellular low-molecular weight thiol, by a process known as *S*-glutathionylation. Protein *S*-glutathionylation may be a critical event in reversal of cysteine oxidation, but may also actively control enzymatic activity, protein-protein interactions, or protein turnover [17,18]. A potential role for *S*-glutathionylation in e.g. epithelial wound responses is indicated by observations of increased overall *S*-glutathionylation at the wound margin of injured epithelial monolayers [19] and impaired cell migration in endothelial cells that overexpress glutaredoxin-1, a major enzyme involved in reversing *S*-glutathionylation [20]. Moreover, *S*-glutathionylation of several specific proteins has been associated with alterations in cell migration dynamics [21–23], although the precise molecular consequences of protein *S*-glutathionylation and the proximal mechanisms that promote *S*-glutathionylation are largely unknown. The present studies were conducted to determine the contribution of DUOX1 in protein *S*-glutathionylation in the context of ATP-mediated epithelial wound responses, and to identify protein targets for DUOX1-dependent *S*-glutathionylation. Our studies reveal the importance of DUOX1 in ATP-stimulated *S*-glutathionylation of a diverse number of proteins, including several key proteins involved in cytoskeletal control, stress responses, and cellular signaling pathways involved in cell migration, and thereby provide additional insights into the mechanistic aspects of DUOX1-mediated epithelial wound responses.

Experimental

Cell culture and treatments

Experiments were performed with a human pulmonary mucoepidermoid carcinoma cell line NCI-H292 (ATCC), which was maintained in RPMI 1640 medium containing 10% fetal bovine serum and 1% penicillin/streptomycin at 37°C and 5% CO_2. To address the role of DUOX1, a stable H292 cell line was generated that was transfected with pRNATin-H1.2/Hygro vector (GenScript, Piscataway, NJ) containing a DUOX1-targeted shRNA sequence (H292-shDUOX1) as well as a corresponding control cell line containing empty vector (H292-CTL). Compared to corresponding controls, H292-shDUOX1 cells are almost completely deficient in DUOX1 mRNA and protein [11]. Additional studies were performed with primary mouse tracheal epithelial (MTE) cells, which were isolated from the tracheas of C57BL/6 J mice (Jackson Laboratories, Bar Harbor, ME) using overnight incubation with 0.1% protease 14 (Sigma-Aldrich, St. Louis, MO) and cultured on rat tail collagen I gel (BD Biosciences, San Jose, CA) in DMEM/F12 media (Invitrogen, Grand Island, NY) supplemented with 20 ng/mL cholera toxin (List Biological Laboratories, Campbell, CA), 10 ng/mL EGF (Calbiochem, San Diego, CA), 5 μg/mL insulin (Sigma), 5 μg/mL transferrin (Sigma), 100 nM dexamethasone (Sigma), 15 μg/mL bovine pituitary extract (Invitrogen), 2 mM L-glutamine, and 50 U/50 μg/mL Penicillin/Streptomycin (Pen/Strep) (Invitrogen), as described previously [24,25]. Similarly, MTE cells were isolated from DUOX1 knockout mice that were originally generated using a retroviral-based gene-trapping method and obtained from Lexicon Pharmaceuticals, Inc. (The Woodlands, TX, USA), and backcrossed onto a C57BL/6J background [26]. Genotypic of DUOX1 knockout mice was performed as described previously [26]. MTE cells were used at passages 2–4.

For experimentation, H292 or MTE cells were seeded at 1×10^5 cells/cm^2 in 24-well plates (BD Labware, Bedford, MA) and cultured for an additional 3–4 days. Prior to cell stimulation, cells were starved overnight in serum-free medium (H292) or EGF-lacking medium (MTE) and stimulated with exogenous ATP (Sigma), and media or cell lysates were collected for the various analyses described below.

Analysis of cellular H_2O_2 production

For analysis of extracellular H_2O_2 production, H292 or MTE cells were seeded in 24 plates and cultured to full confluence (~150,000 cells/well), and after replacing media with 200 μL HBSS, cells were stimulated with ATP and conditioned media was removed at indicated times and mixed with 10 μg/ml lactoperoxidase (Sigma) and 1 mM tyrosine for 15 min, and resulting dityrosine production was analyzed by HPLC as a measure of H_2O_2 production [11]. Alternatively, H_2O_2 in conditioned media was analyzed using the Amplex Red assay (Invitrogen) according to the manufacturer's instructions. Specificity for H_2O_2 was verified by sample pretreatment with catalase (2000 U/ml; Sigma), and H_2O_2 production was calculated using similar analysis of exogenous standards of H_2O_2 in HBSS, and expressed as nmol/10^6 cells. Cellular production of reactive oxygen species was determined 15-min pre-loading of H292 cells or MTE cells in chamber slides with 10 μM 2′,7′-dichlorodihydrofluorescein diacetate (H_2DCF-DA), and visualization of DCF fluorescence as an indicator of cellular oxidant production in response to cell stimulation with ATP, using a Nikon Eclipse E800 fluorescence microscope.

Analysis of cell migration

H292 cells or MTE cells were seeded on fibronectin-coated polycarbonate tissue culture inserts (8-μm pore-size; NUNC) at 1×10^5 cells/well, and incubated for 6 h, after which media with non-attached cells was removed, and cells were further incubated in the absence or presence of ATP for an additional 24 h for analysis of epithelial cell migration by haplotaxis, as previously described [9].

Quantitative analysis of protein S-glutathionylation

Protein *S*-glutathionylation was determined as previously described [27], with some modifications. Briefly, stimulated or unstimulated H292 or MTE cells were lysed in RIPA buffer containing of 50 mM *N*-ethyl maleimide, and cell lysates containing 1 mg protein were precipitated with TCA (6% final concentration), and protein pellets were washed 3x with 1.5% TCA and resuspended in 1 ml of 0.2 M potassium phosphate buffer containing 1 mM EDTA. Aliquots (300 μl) of this final protein solution were adjusted to pH 8.2–8.4 with NaOH and mixed with DTT

(7 mM final concentration) to reduce PSSG to GSH, which was subsequently derivatized for HPLC analysis by mixing (1:1) with 40 mM monobromobimane (mBrB; Calbiochem) in CH_3CN for 15 min. After protein precipitation with TCA (5%), GSH-mBrB was quantified by HPLC with fluorescence detection, as described previously [28]. Control samples were processed similarly without addition of DTT. GSH concentrations were determined using exogenous standards, and PSSG was expressed as nmol/mg protein.

Analysis of protein S-glutathionylation after cell loading with BioGEE

Biotinylated glutathione ethyl ester (BioGEE) was prepared by reacting 0.5 M glutathione ethyl ester (Sigma) with 0.5 M EZ-link sulfo-NHS-biotin (Pierce) in 50 mM $NaHCO_3$ (pH 8.5) as described previously [29], and was added to H292 cells or MTE cells at a final concentration of 250 μM for 1 h, prior to cell treatment with or without ATP for 10 min. After treatment, cells were placed on ice and washed with cold PBS containing 50 mM *N*-ethylmaleimide (NEM) to remove unreacted BioGEE and lysed in 1.5 ml RIPA buffer containing 50 mM NEM. Cell lysates were mixed 1:1 with by non-reducing sample buffer for separation by SDS-PAGE, transferred to PVDF membranes and blotted with streptavidin-HRP to detect biotin-labeled proteins. For identification of biotinylated proteins by Western blot, cleared cell lysates were centrifuged on G25 columns to remove excess biotinylating agent, and biotinylated proteins were collected with high capacity neutravidin beads (Pierce) by constant rotation overnight at 4 °C. Neutravidin beads were washed 4x with RIPA buffer and 2x with PBS containing 1% SDS, after which biotinylated proteins were eluted from the beads by 30 min incubation with PBS containing 1% SDS and 10 mM DTT at room temperature. Eluted protein and corresponding whole cell lysates (as input controls) were mixed with reducing sample buffer for analysis by SDS-PAGE, transferred to PVDF, and blotted with using antibodies against β-actin (Cell Signaling), peroxiredoxin 1 (Prx1; Abcam), c-Src (L4A1; Cell Signaling), and MAPK phosphatase 1 (MKP-1; Santa Cruz). Primarily antibodies were probed with rabbit or mouse-specific secondary antibodies conjugated with HRP (Cell Signaling) and detected by enhanced chemiluminescence (Pierce).

Identification of S-glutathionylated proteins by LC–MS/MS

Confluent H292 cells in 100 mm dishes were preloaded with BioGEE and stimulated with ATP (100 μM) as described above, and cell lysates containing 2.5 mg protein were applied to G25 columns to remove unreacted BioGEE and high-capacity neutravidin (250 μl; Pierce) to collect biotinylated proteins, which were eluted with 10 mM dithiothreitol (DTT) and samples from untreated or ATP-stimulated cells were separated by 1-dimensional SDS-PAGE. After protein visualization by silver staining, each gel lane was cut into small 3–4 mm gel pieces (for a total of 20 pieces per gel lane), which were transferred to microcentrifuge tubes, and washed with 250 μl H_2O for 15′, destained, and dried in a Speed Vac. Proteins in each gel piece were reduced in 200 μl 10 mM DTT in 100 mM NH_4HCO_3 for 1 h at 56 °C, and subsequently incubated in 55 mM iodoacetamide in 100 mM NH_4HCO_3 in the dark for 45′ at room temperature. After removal of iodoacetamide, gel pieces were washed with 100 mM NH_4HCO_3 and dehydrated with 100 μl CH_3CN for 10′, which was repeated once, after which dehydrated gel pieces were dried in a Speed Vac, and re-swelled with trypsin (Promega V511A, 5–20 μg/ml; to achieve trypsin:protein ratio of 1:20 to 1:100 w/w) at 4 °C for 30′, and subsequently incubated overnight at 37 °C for complete protein digestion. Peptides were extracted with 5% formic acid (FA) and 50% acetonitrile, dried and kept in the freezer until LC–MS/MS analysis. The dried peptides were reconstituted with 2.5% CH_3CN/2.5% formic acid and analyzed by capillary LC–MS/MS on an linear ion trap (LTQ) mass spectrometer coupled to a Surveyor MS Pump Plus (Thermo Fisher Scientific, MA). Half of the digest was loaded directly onto a 100 μm × 120 mm capillary column packed with MAGIC C18 (5 μm particle size, 20 nm pore size, Michrom Bioresources, CA) at a flow rate of 500 nL/min, and peptides were separated by a gradient of 3–40% CH3CN/0.1% FA over 30 min, 40–100% CH_3CN/0.1% FA in 1 min, and 100% CH_3CN/0.1% FA in 10 min. Peptides were introduced into the linear ion trap via a nanospray ionization source. Mass spectrometry data was acquired in a data-dependent acquisition mode in which a survey scan from m/z 360–1600 was followed by 10 MS/MS scans of the most abundant ions. Dynamic exclusion was enabled (repeat count: 2; repeat duration: 30 s; exclusion list size: 180; exclusion duration: 60 s). The minimum threshold was 500.

Production spectra were searched against the human subset of the International Protein Index (IPI) database (ver.3.87) containing sequences in forward and reverse orientations using the SEQUEST and MASCOT search engines embedded in the Proteome Discoverer 1.3 (Thermo Fisher Scientific, MA). The 20 raw files from "Control" and "ATP" were processed as one contiguous input file and a single result file was generated. The database was indexed with the following: fully enzymatic activity and two missed cleavage sites allowed for trypsin; peptides MW of 350–5000 Da. Search parameters were as follows: mass tolerance of 2 Da and 0.8 Da for precursor and fragment ions, respectively; four differential PTMs allowed per peptide; dynamic modification on methionine (+15.9949 Da for oxidized methionine) and static modification on cysteine (+57.0215 Da for carbamidomethylated cysteine). Cross-correlation (XCorr) and MASCOT significance filters were applied to limit the false positive (FP) rates to less than 1% in the data sets. ("CNTL" – XCorr: 2.51(1+), 3.04 (2+), 3.68 (3+), 3.695 (4+); significance threshold: 0.020 (Ion Score: 44); "ATP" – XCorr: 2.31(1+), 2.97 (2+), 3.65 (3+), 3.66 (4+); significance threshold: 0.012 (Ion Score: 47)). All the sequence information exported from the Proteome Discoverer msf result files (< 1% FP; with protein grouping enabled) are included as Supplementary information (Supplementary Tables 1 (CNTL) and 2 (ATP)). The search results were further analyzed using Scaffold 4.0.5 (Proteome Software, OR) to compare the unique peptide counts between "Control" and "ATP" with respect to specific protein isoforms/clusters. The following filtering criteria: (1) XCorr: 2.31(1+), 2.97 (2+), 3.65 (3+), 3.66 (4+); and Delta $C_n > 0.1$; (2) MASCOT Ion Score > 44, and (3) "min # of peptide" = 2, were used to achieve a 0% Decoy FDR at the peptide and protein level in the filtered dataset. The "total unique peptide counts" of proteins identified (with keratins removed) are presented in Table 1.

Data analysis and statistics

Quantitative data are presented as mean ± S.E. and statistical differences were determined using Student's *t*-test and differences were considered significant at $p < 0.05$.

Results

DUOX1 activation mediates ATP-dependent H_2O_2 production and protein S-glutathionylation

We first confirmed the importance of DUOX1 in cellular H_2O_2 production response to extracellular ATP, using two separate epithelial cell models, namely human airway epithelial H292 cells and mouse tracheal epithelial (MTE) cells. As shown in Fig. 1A, stimulation of H292 cells with ATP induced rapid and transient

Table 1
Proteins identified in unstimulated (CNTL) and ATP stimulated H292 cells.

	Protein name	Accession number	M.W. (kDa)	No. of peptides	
				CNTL	ATP
1	**Cluster of Uncharacterized protein (IPI00022434)**				
1.1	Uncharacterized protein	IPI00022434	72	8	6
1.2	Uncharacterized protein	IPI00878517	56	6	4
2	**Cluster of Isoform DPI of Desmoplakin (IPI00013933)**				
2.1	Isoform DPI of Desmoplakin	IPI00013933	332	12	13
2.2	Desmoplakin Ia	IPI00969616	279	10	12
2.3	cDNA FLJ61543, highly similar to Desmoplakin	IPI01009332	156	9	8
2.4	cDNA FLJ26719 fis, clone PNC03379	IPI00746877	20	0	0
3	**Desmoglein-1**	IPI00025753	114	5	10
4	**Cluster of actin, cytoplasmic 1 (IPI00021439)**				
4.1	Actin, cytoplasmic 1	IPI00021439 (+1)	42	4	7
4.2	Isoform 1 of POTE ankyrin domain family member E	IPI00479743	121	2	2
4.3	Putative beta-actin-like protein 3	IPI00888712	42	0	0
4.4	POTE ankyrin domain family member I	IPI00740545	121	0	0
4.5	cDNA FLJ52761, highly similar to Actin, aortic smooth muscle	IPI00984879	37	2	0
4.6	POTE ankyrin domain family member J	IPI00738655	117	0	0
4.7	Actin, alpha skeletal muscle	IPI00021428	42	3	3
4.8	POTE ankyrin domain family member F	IPI00739539	121	2	2
4.9	Uncharacterized protein	IPI00645534	17	2	2
4.10	cDNA FLJ52755, highly similar to Actin, aortic smooth muscle	IPI00921887	17	2	2
4.11	Uncharacterized protein	IPI00917820	16	2	2
4.12	Uncharacterized protein	IPI00917545	6	0	0
4.13	Actin-like protein (Fragment)	IPI00970910	11	0	0
4.14	Similar to Kappa-actin	IPI00893501	5	0	0
4.15	Actin-like protein (Fragment)	IPI00970912	12	0	0
4.16	Uncharacterized protein	IPI00917282	11	0	0
5	**Cluster of Heat shock protein HSP 90-beta (IPI00414676)**				
5.1	Heat shock protein HSP 90-beta	IPI00414676	83	5	9
5.2	Heat shock protein 90Bb	IPI00455599	49	0	3
5.3	Isoform 2 of Heat shock protein HSP 90-alpha	IPI00382470 (+1)	98	0	9
5.4	Putative heat shock protein HSP 90-beta 4	IPI00555565	58	0	2
5.5	Putative heat shock protein HSP 90-alpha A2	IPI00031523	39	0	3
5.6	Uncharacterized protein	IPI00604607	49	0	7
5.7	Uncharacterized protein	IPI00514027	19	0	0
6	**Junction plakoglobin**	IPI00554711	82	5	9
7	**Cluster of Isoform 2 of Filamin-A (IPI00302592)**				
7.1	Isoform 2 of Filamin-A	IPI00302592 (+2)	280	0	8
7.2	Protein	IPI00893150	10	0	0
7.3	Filamin A, alpha	IPI01018650	25	0	0
8	**Cluster of cDNA FLJ56442, highly similar to ATP-citrate synthase (IPI00394838)**				
8.1	cDNA FLJ56442, highly similar to ATP-citrate synthase	IPI00394838	125	5	15
8.2	ATP-citrate synthase	IPI00021290	121	5	15
9	**Hornerin**	IPI00398625	282	7	3
10	**Cluster of Glyceraldehyde-3-phosphate dehydrogenase (IPI00219018)**				
10.1	Glyceraldehyde-3-phosphate dehydrogenase	IPI00219018	36	3	4
10.2	Glyceraldehyde-3-phosphate dehydrogenase	IPI00795257	32	3	4
10.3	Glyceraldehyde-3-phosphate dehydrogenase	IPI00789134	28	2	3
11	**Cluster of Isoform 1 of Myosin-9 (IPI00019502)**				
11.1	Isoform 1 of Myosin-9	IPI00019502	227	6	13
11.2	FLJ00279 protein (Fragment)	IPI00742780	66	3	3
11.3	Uncharacterized protein	IPI00556012	25	0	0
12	**Cluster of Isoform 2 of Annexin A2 (IPI00418169)**				
12.1	Isoform 2 of Annexin A2	IPI00418169	40	4	4
12.2	Putative annexin A2-like protein	IPI00334627	39	3	3
12.3	cDNA FLJ34687 fis, clone MESAN2000620, highly similar to Annexin A2	IPI00903334	21	2	2
13	**Filaggrin-2**	IPI00397801	248	5	2
14	**Cluster of 88 kDa protein (IPI01026194)**				
14.1	88 kDa protein	IPI01026194	88	0	0
14.2	Uncharacterized protein	IPI00645452 (+4)	48	0	4
14.3	Similar to Tubulin beta-2A chain	IPI00975573	24	0	0
14.4	TUBB6 protein	IPI00646779	50	0	0
14.5	Tubulin beta-8 chain B	IPI00174849	50	0	0
14.6	Tubulin beta-4 chain	IPI00023598	50	0	2
14.7	Putative uncharacterized protein (Fragment)	IPI00827736	17	0	0
14.8	Tubulin beta 2C (Fragment)	IPI00956734	10	0	0
14.9	Putative tubulin beta-4q chain	IPI00018511	48	0	0
15	**Cluster of Hemoglobin subunit beta (IPI00654755)**				
15.1	Hemoglobin subunit beta	IPI00654755 (+1)	16	0	4
15.2	Hbbm fused globin protein (Fragment)	IPI00930351	11	0	2
15.3	Hemoglobin subunit gamma-2	IPI00554676	16	0	0
15.4	Hemoglobin subunit epsilon	IPI00217471	16	0	0
16	**Dermcidin**	IPI00027547	11	3	3

Table 1 (*continued*)

	Protein name	Accession number	M.W. (kDa)	No. of peptides	
				CNTL	ATP
17	**Cluster of Uncharacterized protein (IPI01015738)**				
17.1	Uncharacterized protein	IPI01015738	80	0	3
17.2	alpha-actinin-1 isoform a	IPI00759776	106	0	4
17.3	cDNA FLJ54718, highly similar to Alpha-actinin-1	IPI01025172	30	0	0
17.4	34 kDa protein	IPI01009456	34	0	2
17.5	Protein	IPI01026210	29		2
18	**Cluster of 268 kDa protein (IPI00942045)**				
18.1	268 kDa protein	IPI00942045	268	0	7
18.2	Uncharacterized protein	IPI01014477	120	0	5
18.3	Isoform 4 of Acetyl-CoA carboxylase 1	IPI00396015	270	0	7
19	**Cluster of Trifunctional enzyme subunit alpha, mitochondrial (IPI00031522)**				
19.1	Trifunctional enzyme subunit alpha, mitochondrial	IPI00031522	83	2	5
19.2	cDNA FLJ52806, highly similar to Trifunctional enzyme subunit alpha, mitochondrial	IPI00908351	28	0	0
20	**Cluster of Pyruvate carboxylase, mitochondrial (IPI00299402)**				
20.1	Pyruvate carboxylase, mitochondrial	IPI00299402	130	0	5
20.2	Uncharacterized protein	IPI00975989	33	0	5
21	**Methylcrotonoyl-CoA carboxylase subunit alpha, mitochondrial**	IPI00024580	80	0	4
22	**myosin-11 isoform SM1B**	IPI00743857	228	0	2
23	**Cluster of Uncharacterized protein (IPI00922694)**				
23.1	Uncharacterized protein	IPI00922694	70	0	4
23.2	Stress-70 protein, mitochondrial	IPI00007765 (+1)	74a	0	4
24	**Cluster of Annexin A1 (IPI00218918)**				
24.1	Annexin A1	IPI00218918	39	0	5
24.2	Uncharacterized protein	IPI00549413	23	0	0
25	**30 kDa protein**	IPI00917420	30	3	2
26	**Fatty acid synthase**	IPI00026781	273	0	2
27	**Cluster of Protein (IPI01012384)**				
27.1	Protein	IPI01012384	124	0	3
27.2	Importin 5	IPI00514205	14	0	0
27.3	Uncharacterized protein	IPI00947399	14	0	0
28	**Isoform 2 of Plakophilin-1**	IPI00071509 (+1)	83	2	2
29	**Cluster of T-complex protein 1 subunit beta (IPI00297779)**				
29.1	T-complex protein 1 subunit beta	IPI00297779	57	0	2
29.2	T-complex protein 1 subunit beta isoform 2	IPI00981169	53	0	0
30	**Cluster of Puromycin-sensitive aminopeptidase (IPI00026216)**				
30.1	Puromycin-sensitive aminopeptidase	IPI00026216	103	2	2
30.2	Protein	IPI00979097	49	0	0
30.3	Uncharacterized protein	IPI00976960	22	0	0
30.4	Uncharacterized protein	IPI00984113	20	0	0
31	**Isoform 2 of Propionyl-CoA carboxylase alpha chain, mitochondrial**	IPI00895869	77	0	4
32	**Cluster of Uncharacterized protein (IPI00964079)**				
32.1	Uncharacterized protein	IPI00964079	57	0	2
32.2	cDNA FLJ59103, highly similar to T-complex protein 1 subunit epsilon	IPI00909956	32	0	2
33	**Cluster of Isoform 1 of Myosin-14 (IPI00337335)**				
33.1	Isoform 1 of Myosin-14	IPI00337335 (+3)	228	0	2
33.2	Isoform 5 of Myosin-14	IPI00029818 (+1)	168	0	0
34	**Cluster of tropomyosin alpha-3 chain isoform 1 (IPI00183968)**				
34.1	tropomyosin alpha-3 chain isoform 1	IPI00183968	33	0	2
34.2	TPM1 protein variant (Fragment)	IPI00940084	34	0	0
34.3	tropomyosin alpha-1 chain isoform 7	IPI00216134	33	0	0
34.4	Isoform 2 of Tropomyosin alpha-4 chain	IPI00216975	33	0	0
34.5	cDNA FLJ16459 fis, clone BRCAN2002473, moderately similar to Tropomyosin, fibroblast isoform 2	IPI00940343	37	0	0
34.6	Isoform 2 of Tropomyosin beta chain	IPI00220709	33	0	0
34.7	Isoform 1 of Tropomyosin alpha-4 chain	IPI00010779	29	0	0
34.8	Isoform 1 of Tropomyosin beta chain	IPI00013991	33	0	0
34.9	Uncharacterized protein	IPI01018017	28	0	0
35	**Cluster of cDNA FLJ53765, highly similar to Tubulin alpha chain (IPI00909762)**				
35.1	cDNA FLJ53765, highly similar to Tubulin alpha chain	IPI00909762	20	0	3
35.2	cDNA FLJ55956, highly similar to Tubulin alpha-6 chain	IPI00387144	58	0	4
35.3	cDNA FLJ53743, highly similar to Tubulin alpha-3 chain	IPI00936821	43	0	0
35.4	Tubulin alpha-4A chain	IPI00007750 (+1)	50	0	2
35.5	Tubulin alpha-3E chain	IPI00410402	50	0	2
35.6	Isoform 1 of Tubulin alpha-3C/D chain	IPI00179709	50	0	2
35.7	Isoform 2 of Tubulin alpha-3C/D chain	IPI00218345	46	0	2
35.8	Similar to Tubulin alpha-3C/D chain	IPI00784332	36	0	0
35.9	Uncharacterized protein	IPI01022794	25	0	0
36	**Isoform 2 of Procollagen-lysine,2-oxoglutarate 5-dioxygenase 2**	IPI00337495	87	0	4
37	**Isoform 1 of Myosin-10**	IPI00397526 (+1)	229	0	2
38	**Exportin-1**	IPI00298961	123	0	2
39	**Ubiquitin-like modifier-activating enzyme 1**	IPI00645078	118	0	2
40	**Cluster of Elongation factor 2 (IPI00186290)**				
40.1	Elongation factor 2	IPI00186290	95	0	2
40.2	Uncharacterized protein	IPI01010856	65	0	0

Table 1 (*continued*)

	Protein name	Accession number	M.W. (kDa)	No. of peptides	
				CNTL	ATP
41	**Cluster of ADP/ATP translocase 3 (IPI00291467)**				
41.1	ADP/ATP translocase 3	IPI00291467	33	0	0
41.2	ADP/ATP translocase 4	IPI00010420	35	0	0
41.3	ADP/ATP translocase 2	IPI00007188	33	0	2
42	**Uncharacterized protein**	IPI00943181	29	0	3
43	**Isoform 1 of Clathrin heavy chain 1**	IPI00024067 (+1)	192	0	3
44	**Cluster of Elongation factor 1-alpha 1 (IPI00396485)**				
44.1	Elongation factor 1-alpha 1	IPI00396485	50	2	0
44.2	Putative elongation factor 1-alpha-like 3	IPI00472724	50	2	0
44.3	Elongation factor 1-alpha 2	IPI00014424	50	2	0
44.4	EEF1A protein (Fragment)	IPI00382804	24	0	0
45	**Cluster of Alpha-amylase 1 (IPI00300786)**				
45.1	Alpha-amylase 1	IPI00300786 (+1)	58	3	0
45.2	58 kDa protein	IPI00646265	58	3	0
46	**Beta-actin-like protein 2**	IPI00003269	42	0	2
47	**Isoform 1 of Glycerol-3-phosphate dehydrogenase, mitochondrial**	IPI00017895	81	0	2
48	**Cluster of cDNA FLJ56389, highly similar to Elongation factor 1-gamma (IPI00000875)**				
48.1	cDNA FLJ56389, highly similar to Elongation factor 1-gamma	IPI00000875 (+1)	56	0	2
48.2	cDNA FLJ59433, highly similar to Elongation factor 1-gamma	IPI00909534	24	0	0
49	**Isoform 1 of Arginase-1**	IPI00291560 (+1)	35	0	2
50	**cDNA FLJ60461, highly similar to Peroxiredoxin-2**	IPI00909207	20	0	2
51	**Cluster of Peroxiredoxin-4 (IPI00011937)**				
51.1	Peroxiredoxin-4	IPI00011937	31	0	3
51.2	Protein	IPI00639945	18	0	3
52	**Dolichyl-diphosphooligosaccharide–protein glycosyltransferase subunit 1 precursor**	IPI00025874	73	0	4
53	**triosephosphate isomerase isoform 2**	IPI00465028 (+1)	31	0	2
54	**Transferrin receptor protein 1**	IPI00022462	85	0	2
55	**Transitional endoplasmic reticulum ATPase**	IPI00022774	89	0	2
56	**CTP synthase 1**	IPI00290142	67	0	2
57	**Isoform 1 of F-actin-capping protein subunit beta**	IPI00026185 (+1)	31	0	2
58	**Cluster of Isoform 2 of Inactive tyrosine-protein kinase 7 (IPI00170814)**				
58.1	Isoform 2 of Inactive tyrosine-protein kinase 7	IPI00170814 (+2)	114	0	2
58.2	PTK7 protein tyrosine kinase 7 isoform a variant (Fragment)	IPI00555762	84	0	0
58.3	Uncharacterized protein	IPI00946128	29	0	0
59	**Cluster of Importin-7 (IPI00007402)**				
59.1	Importin-7	IPI00007402	120	0	2
59.2	Uncharacterized protein	IPI00981775	15	0	0
60	**Cluster of Isoform 2 of Voltage-dependent anion-selective channel protein 3 (IPI00294779)**				
60.1	Isoform 2 of Voltage-dependent anion-selective channel protein 3	IPI00294779	31	0	2
60.2	Uncharacterized protein	IPI00981487	18	0	0
61	**cDNA FLJ39276 fis, clone OCBBF2010843, highly similar to Guanine nucleotide-binding protein G(i), alpha-2 subunit**	IPI00925504	39	0	2
62	**Isoform 3 of Tropomyosin alpha-3 chain**	IPI00218320 (+1)	29	0	2
63	**Conserved hypothetical protein**	IPI00978107	22	0	2

One of the protein members in the cluster is assigned by Scaffold to represent the corresponding cluster.

increase in extracellular H_2O_2 production, which was maximal at 10–15 min and gradually declined thereafter, indicating transient activation of DUOX1 by ATP-dependent purinoceptor stimulation. Moreover, ATP-induced extracellular H_2O_2 production was dramatically attenuated in H292 cells lacking DUOX1 due to transfection with DUOX1-targeted shRNA (H292-shDUOX1) [11] (Fig. 1B). Equivalent findings were obtained using the Amplex Red assay (results not shown). Complementary studies with primary MTE cells from wild-type C57BL/6J mice similarly showed increased H_2O_2 production in response to ATP stimulation, albeit at markedly lower levels compared to similar stimulation of H292 cells, and this also requires DUOX1 since it was not observed using MTE cells obtained from DUOX1 knockout mice [26] (Fig. 1C). Comparative analysis of cellular oxidant production in response to ATP, using cell preloading with the oxidant-sensitive probe H_2DCF, similarly indicated markedly increased oxidant production in ATP-stimulated cells from wild-type mice compared to DUOX1-knockout mice (Fig. 1D).

To determine whether ATP-dependent DUOX1 activation promotes protein *S*-glutathionylation as a mechanism of redox signaling, we quantified the overall cellular levels of *S*-glutathionylated proteins (PSSG) in response to ATP stimulation. As shown in Fig. 2A, ATP stimulation of H292 cells caused a rapid increase in overall PSSG levels, which reached an optimum 10–15 min after ATP stimulation and decreased at later time points, kinetics resembling transient DUOX1 activation (Fig. 1A) and suggesting the importance of DUOX1 in PSSG formation. Accordingly, no increase in protein PSSG levels were observed in ATP-stimulated H292-shDUOX1 cells (Fig. 2B). Similar results were obtained in MTE cells, which showed significant increases in PSSG in response to ATP stimulation, only in MTE cells from wild-type mice but not from DUOX1-KO mice (Fig. 2C). ATP-stimulated increases in overall protein *S*-glutathionylation were not associated with significant changes in overall GSH redox status, determined by analysis of GSH/GSSG ratios [30] (results not shown), indicating that DUOX1-dependent protein *S*-glutathionylation was most likely induced by initial oxidation of target protein cysteines rather than protein S-glutathionylation via initial formation of GSSG.

Identification of S-glutathionylated proteins by LC–MS/MS

As an alternative approach to demonstrate protein *S*-glutathionylation, and a means to identify protein targets for glutathionylation,

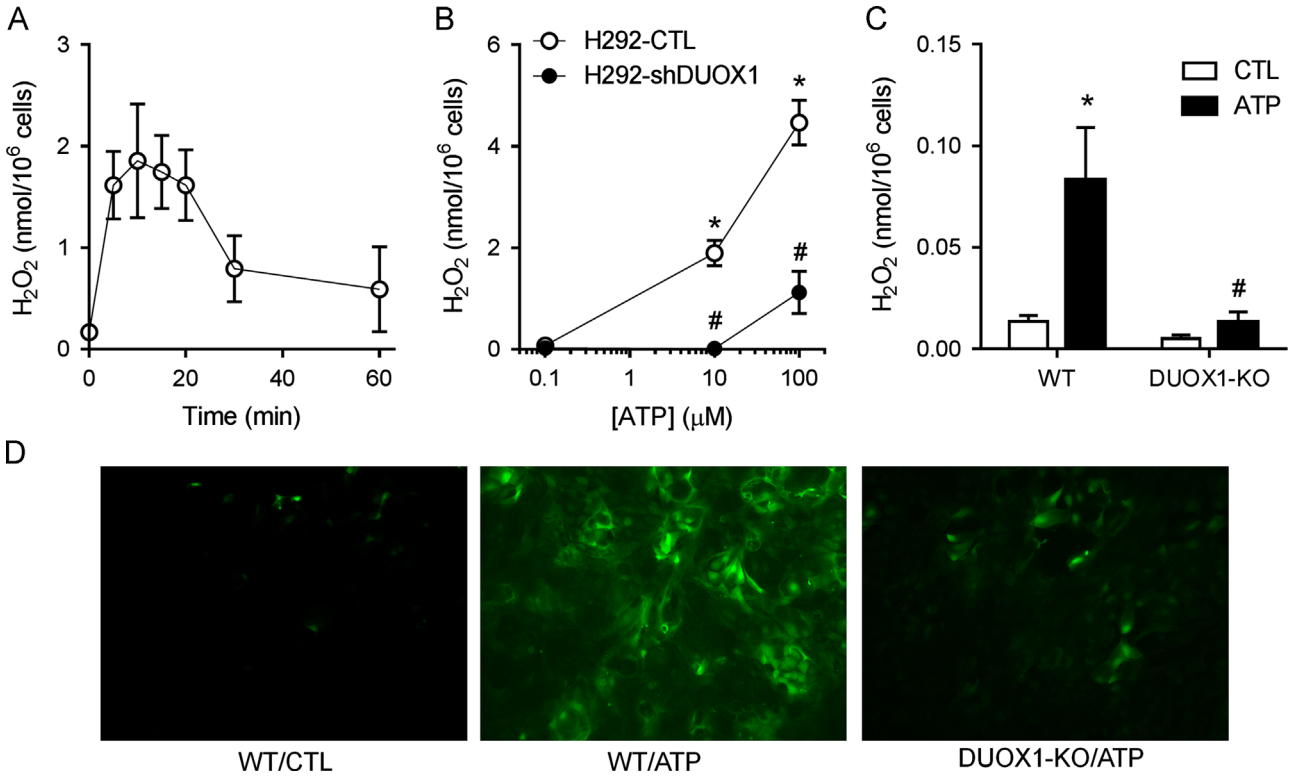

Fig. 1. ATP-stimulated oxidant production originates from DUOX1. (A) H292 cells were stimulated with 100 μM ATP for indicated times and H_2O_2 levels in conditioned media were determined by HPLC. Mean ± S.E. from 4 replicates are shown. (B) Dose-dependent production of extracellular H_2O_2 after 15-min ATP stimulation of DUOX1 shRNA transfected H292 cells (H292-shDUOX1) and corresponding control transfectants (H292-CTL). Mean ± S.E. from 4 replicates in 2 separate experiments. (C) ATP-stimulated production of extracellular H_2O_2 after 15-min stimulation of MTE cells from wild-type (WT) or DUOX1-deficient (DUOX1-KO) mice with 100 μM ATP. Mean ± S.E ($n=3$). : $p<0.05$ compared to unstimulated control; #: $p<0.05$ compared to corresponding treatment of H292-CTL or WT MTE cells. (D) Analysis of cellular oxidant production by DCF fluorescence. MTE cells from either wild-type (WT) or DUOX1-deficient (DUOX1-KO) mice were preloaded with H_2DCF-DA (10 μM, 15′), and stimulated with 100 μM ATP and DCF fluorescence was visualized after 15 min. Representative images of 3 separate analyses are shown.

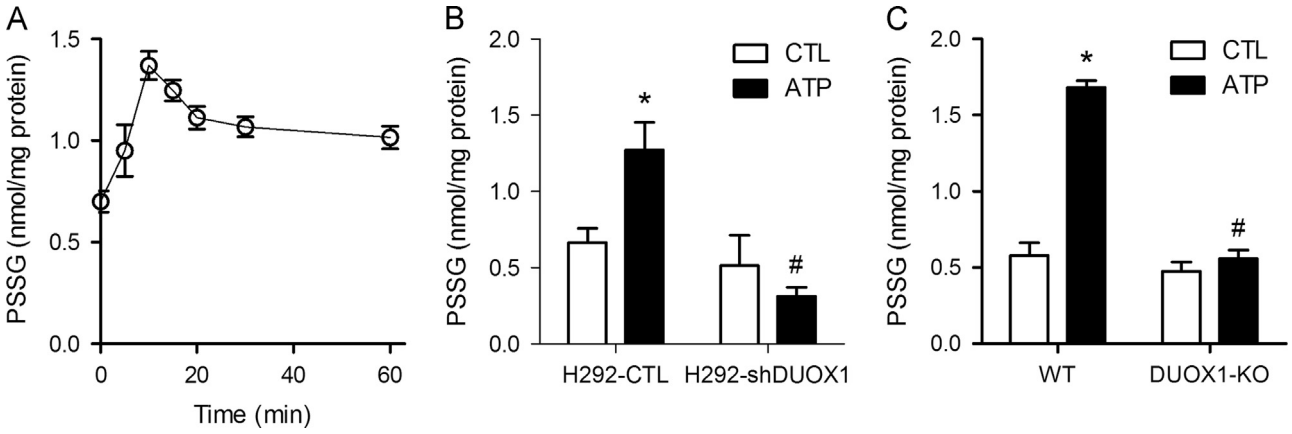

Fig. 2. DUOX1 activation promotes protein *S*-glutathionylation. (A) H292 cells were stimulated with 100 μM ATP for the indicated periods of time, after which cells collected in lysis buffer containing 50 mM NEM. Protein lysates were precipitated with TCA and incubated with DTT to reduce protein mixed disulfides with GSH (PSSG), and GSH was analyzed by HPLC after mBrB derivatization. (B) Analysis of PSSG in unstimulated or ATP-stimulated (100 μM; 15 min) H292-CTL or H292-shDUOX1 cells. (C) PSSG analysis in unstimulated or ATP stimulated MTE cells from wild-type (WT) or DUOX1-deficient (DUOX1-KO) mice. Mean ± S.E. from 4 replicates in 2 separate experiments. : $p<0.05$ compared to unstimulated control; #: $p<0.05$ compared to corresponding treatment of H292-CTL cells.

H292 cells or MTE cells were pre-loaded with BioGEE prior to cell stimulation with ATP, after which protein *S*-glutathionylation was assessed by incorporation of biotin. Analysis of H292 cell lysates by non-reducing SDS-PAGE and streptavidin blotting revealed that ATP stimulation resulted in increased biotinylation of a number of proteins, whereas minimal increases in biotin incorporation were observed in similarly stimulated H292-shDUOX1 cells (Fig. 3A), confirming the involvement of DUOX1 in ATP-stimulated protein *S*-glutathionylation. Similar analysis of protein *S*-glutathionylation in BioGEE-loaded MTE cells from wild-type mice and DUOX1-deficient mice yielded comparable results (Fig. 3B), illustrating a critical role for DUOX1 in enhanced *S*-glutathionylation of a variety of proteins in response to cell stimulation with exogenous ATP.

To identify protein targets for *S*-glutathionylation in response to ATP stimulation, biotinylated proteins from BioGEE-loaded H292 cells were purified with avidin chromatography and separated by 1-dimensional SDS-PAGE, after which each gel lane was cut into 20 sections for in-gel protein digestion with trypsin for analysis by LC-MS/MS. Selection criteria for positive protein identification included representation by at least 2 unique

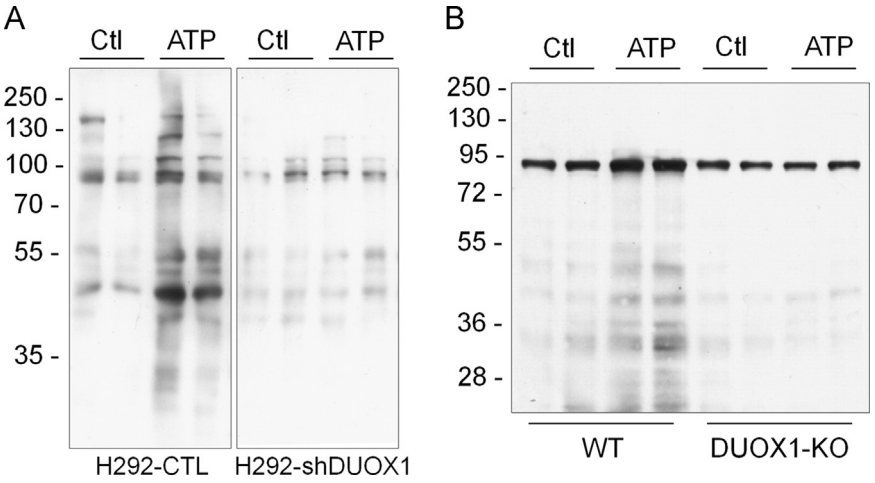

Fig. 3. Analysis of DUOX1-dependent protein *S*-glutathionylation using BioGEE. H292-CTL or H292-shDUOX1 cells (A) or MTE cell from either wild-type or DUOX1 knockout mice (B) were preloaded with BioGEE (250 μM; 1 h), stimulated with ATP (100 μM; 15 min), and cell lysates were mixed with non-reducing sample buffer for analysis by SDS-PAGE, and biotin-labeled proteins were detected by blotting with streptavidin-HRP and enhanced chemiluminescence. Representative blots of 2–3 independent experiments are shown.

peptides, and keratins were excluded from the data set. As illustrated in Table 1, 19 *S*-glutathionylated proteins were identified in unstimulated H292 cells, and this number increased to 61 in ATP-stimulated cells. Sequence information for the proteins identified in control and ATP-stimulated samples is presented in Supplementary Tables S1 and S2. A number of *S*-glutathionylated proteins (44) were detected only in ATP-stimulated H292 cells but not in controls, indicating that these proteins are *S*-glutathionylated in response to ATP stimulation. In addition, among the *S*-glutathionylated proteins that were identified in both unstimulated and ATP-stimulated cells, they were in several cases represented by a greater number of detected tryptic peptides, suggesting increased protein abundance and thus increased *S*-glutathionylation of these proteins. Other identified proteins in both samples likely reflect proteins that are *S*-glutathionylated by mechanisms independent of ATP stimulation and DUOX1 activation. Targets for ATP-dependent *S*-glutathionylation include proteins in several functional categories, including cytoskeletal proteins, heat shock proteins, and proteins involved in metabolism or redox regulation (Table 1).

DUOX1-dependent S-glutathionylation of proteins involved in cell migration

Previous studies have indicated an important role for extracellular ATP in epithelial wound responses by promoting DUOX1-dependent cell migration [11,12], and cell migration is also associated with increased protein *S*-glutathionylation [19,20]. We therefore established the importance of DUOX1 in ATP-dependent *S*-glutathionylation of several selected proteins that have previously been invoked in cell migration, by Western blot analysis of biotin-labeled proteins from BioGEE-loaded stimulated or unstimulated H292 or MTE cells. As expected, ATP-stimulated migration of H292 cells as well as MTE cells depended critically on DUOX1, as this response was suppressed completely in H292-shDUOX1 cells and DUOX1-deficient MTE cells (Fig. 4A and B). Western blot analysis of biotinylated proteins from BioGEE-preloaded H292 cells showed ATP-dependent increases in *S*-glutathionylation of several proteins with known functions in cytoskeletal regulation or cell migration, namely β-actin, Prx-1, Src, and MKP-1 (Fig. 4C). Moreover, no such increases were observed in H292-shDUOX1 cells that lack DUOX1 (Fig. 4C), indicating that ATP-dependent *S*-glutathionylation of these proteins is DUOX1-dependent and may represent key events in promoting cell motility and migration. Similar findings were observed in MTE cells, in which ATP stimulation promoted *S*-glutathionylation of these proteins cells from wild-type mice but not from DUOX1 knockout mice (Fig. 4D). Collectively, these findings confirm that DUOX1 activation contributes to ATP-stimulated epithelial cell migration at several levels, by promoting *S*-glutathionylation of a number of target proteins involved in cell signaling and cytoskeletal control.

Discussion

The present studies build on our recent studies that indicate a role of DUOX1 in epithelial wound responses, and highlight the involvement of *S*-glutathionylation of a number proteins as a potential key mechanism in these responses. Wound healing is a complex and essential biological process that involves both immediate actions of conserved damage signals as well as transcription of a variety of genes to further advance the wound response, and a range of studies in diverse organisms and cell systems have identified the common involvement of purinergic molecules (including as ATP), Ca^{2+}, and reactive oxygen species such as H_2O_2, as mediators in early wound responses [31]. Previous studies with airway epithelial cells have demonstrated a transient rise in extracellular ATP in response to cell activation or injury [12,32], and in turn, the present studies demonstrate rapid and transient activation of DUOX1-dependent H_2O_2 production in airway epithelial cells in response to extracellular ATP, which is in close agreement with recently reported transient and localized H_2O_2 generation in injured tail fin of zebrafish larvae [7]. While the overall importance of H_2O_2 in wound healing responses has been well recognized [31], the direct targets of H_2O_2-dependent oxidation during wound healing remain to be fully identified. Using both human and mouse epithelial cell model systems, we herein demonstrate the critical importance of DUOX1 in promoting *S*-glutathionylation of several target proteins in response to cell stimulation with extracellular ATP. Using a global proteomic survey and targeted analysis of candidate proteins, our studies reveal that ATP stimulation and/or DUOX1 activation promotes the *S*-glutathionylation of a diverse range of proteins involved in either cytoskeletal control, cell metabolism, and redox signaling, and indicating that ATP- and DUOX1-mediated wound responses are not due to a single redox event, but rather involve concerted and integrated redox regulation of a range of proteins.

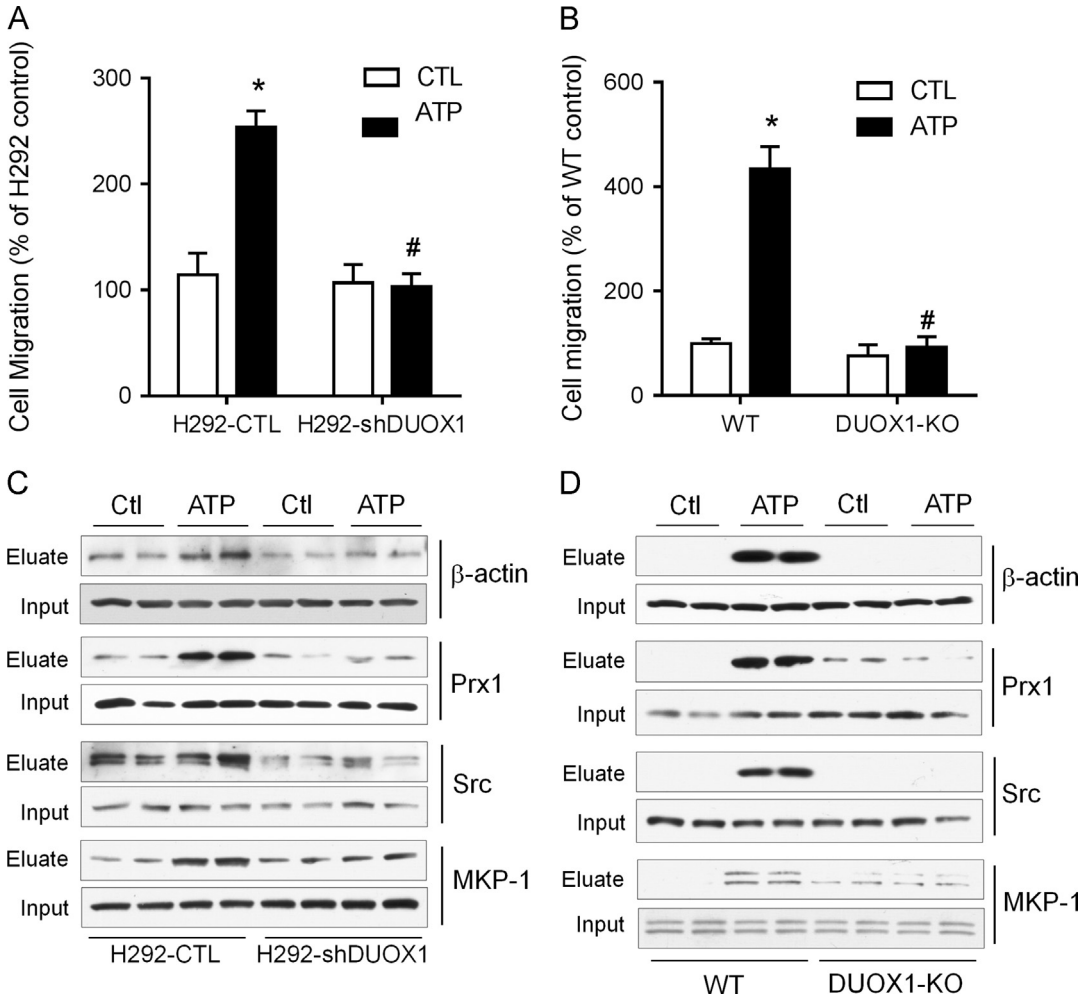

Fig. 4. DUOX1 activation promotes *S*-glutathionylatoin of proteins involved in cell migration. H292-CTL and H292-shDUOX1 cells (A) or MTE cells from wild-type (WT) or DUOX1-deficient (DUOX1-KO) mice (B) were seeded on 8 μm polycarbonate filters coated with fibronectin and cell migration by haptotaxis was evaluated in the absence or presence of ATP (100 μM) over 24 h, and quantified and expressed relative to unstimulated H292 cells. Mean S.E. ($n=4$). : $p<0.05$ compared to unstimulated control; #: $p<0.05$ compared to corresponding treatment of H292-CTL or WT MTE cells. BioGEE-preloaded H292-CTL or H292-shDUOX1 cells (C) or MTE cells from WT or DUOX1-KO mice (D) were stimulated with ATP and biotinylated proteins were collected using neutravidin beads, and analyzed by SDS-PAGE and Western blotting with antibodies against β-actin, Prx1, MKP-1, or Src. Corresponding whole cell lysates were evaluated as input controls. Representative blots of 2 independent experiments are shown.

In spite of the variable extent of ATP-dependent extracellular H_2O_2 production by H292 cells compared to MTE cells (Fig. 1), the overall extent of ATP-stimulated protein *S*-glutathionylation was comparable (Figs. 3 and 4). In fact, our findings indicate that the extent of ATP-dependent *S*-glutathionylation corresponds poorly with extracellular H_2O_2 production, which merely reflects H_2O_2 production at the cell surface rather than overall cellular H_2O_2. Indeed, it is important to note that a substantial fraction DUOX protein is localized to intracellular compartments [14], and that ATP-dependent protein *S*-glutathionylation may have resulted primarily from *intracellularly* produced H_2O_2 or related oxidant species (as indicated by DCF fluorescence; Fig. 1D), rather than paracrine effects of extracellularly generated H_2O_2. It is also important to consider that cellular oxidant production in response to ATP may not exclusively originate from DUOX1, but may also involve additional sources such as mitochondria, as an example of previously established cross-talk between NADPH oxidases and mitochondria with respect to oxidant production and redox signaling [33,34]. Indeed, ATP-dependent purinergic activation not only results in activation of DUOX1 or other NADPH oxidases, but also evokes cellular responses due to activation of mitochondria-derived reactive oxygen species (e.g. [35]). Intriguingly, our present proteomic analyses indicate that ATP stimulation resulted in markedly increased *S*-glutathionylation of several mitochondrial proteins, such as pyruvate carboxylase or ATP-citrate synthase (Table 1), which would suggest involvement of mitochondria-derived oxidants. The almost complete inhibition of ATP-dependent oxidant production as well as overall *S*-glutathionylation in cells lacking DUOX1 would suggest that such mitochondrial oxidant production and *S*-glutathionylation of mitochondrial proteins may have resulted from initial activation of DUOX1, although this remains to be formally tested in future studies.

Using Western blotting of biotin-labeled proteins in BioGEE-loaded cells, we demonstrated DUOX1-dependent *S*-glutathionylation of several proteins with known roles in cell signaling and cytoskeletal regulation in response to ATP stimulation. For example, dynamic alterations of the actin cytoskeleton and localized formation of actin filaments at the leading edge are critical for cell migration [36], and a critical cysteine residue in actin, Cys374, was recently identified as a target for reversible *S*-glutathionylation upon cell stimulation or during cell adhesion [37,38]. Our observation of DUOX1-dependent actin *S*-glutathionylation in response to ATP stimulation of airway epithelial cells would suggest that such actin *S*-glutathionylation similarly controls cytoskeletal dynamics and promotes cell migration dynamics. The importance of the dynamics of actin *S*-glutathionylation and de-glutathionylation in cell migration was recently demonstrated in studies with neutrophils lacking glutaredoxin 1

(Grx1), which displayed enhanced actin *S*-glutathionylation in response to neutrophil activation that was associated with reduced neutrophil polarization, chemotaxis, adhesion, and phagocytosis [21].

Another target for DUOX1-dependent *S*-glutathionylation is the MAPK phosphatase MKP-1, which controls MAPK signaling pathways involved in cell motility and migration [12]. Indeed, recent studies in monocytes demonstrated that *S*-glutathionylation of MKP-1 results in its inactivation and subsequent degradation, thereby promoting monocyte adhesion and migration [22], and suggest that DUOX1-dependent MKP-1 *S*-glutathionylation might similarly promote epithelial cell migration. Additionally, following recent studies demonstrating a critical role for oxidative activation of Src family kinases in DUOX-dependent cell migration [9,11], our present findings suggest that such oxidative activation of Src may involve *S*-glutathionylation. Finally, reversible *S*-glutathionylation is also known to regulate the functions of peroxiredoxins, a family of ubiquitously expressed thiol-specific peroxidase enzymes. Of the various Prx isoforms, Prx1 appears to be particularly sensitive to *S*-glutathionylation, especially at Cys83, preventing its functional change from low molecular weight oligomers with peroxidase activity to high molecular weight complexes that possess molecular chaperone activity [39,40]. DUOX1-dependent Prx1 *S*-glutathionylation may be critical important in preserving its peroxidase properties to regulate appropriate redox signaling. The involvement of Prx1 in controlling NADPH oxidase-dependent redox signaling and wound responses is supported by recent studies demonstrating transient inactivation of Prx1 by Src-dependent phosphorylation [41]. In addition, Prx1 was also recently demonstrated to interact with MAPK phosphatases such as MKP-1 to control cell signaling pathways [42]. Collectively, the apparent involvement of DUOX1 in *S*-glutathionylation of these various protein targets, and their known interactions in various cellular processes suggests DUOX1-dependent redox regulation of these processes at various levels as illustrated in Fig. 5. However, the precise cysteine targets for DUOX1-derived H_2O_2 in these proteins are still unclear, as are the functional consequences of their oxidation, and this will need to be established in future studies.

In summary, the present studies establish an important role for DUOX1 in cellular redox signaling by protein *S*-glutathionylation, and identify a number of protein targets that are subject to DUOX1-dependent *S*-glutathionylation in response to ATP, with known functions in cytoskeletal control and cell migration, cell metabolism, and redox regulation. It is important to recognize that our global proteomic survey has some limitations, as it may have failed to detect some putative *S*-glutathionylation targets, and conversely may have generated some false positives (e.g. resulting from co-purification with biotin-tagged proteins), and their definitive identification as *S*-glutathionylated proteins would require complementary approaches. The diverse nature of protein targets for DUOX1-dependent *S*-glutathionylation is consistent with recent studies indicating NOX/DUOX-dependent H_2O_2 gradients that may act by paracrine signaling e.g. as a chemotactic signal to recruit neutrophils and macrophages to wound sites by more distant redox events [7,16]. However, our present findings to not establish whether identified *S*-glutathionylated proteins are direct targets for DUOX1-derived H_2O_2 and we can not rule out the possibility that some of these may have been *S*-glutathionylated by more indirect mechanisms, e.g. by indirect oxidant production by mitochondria [35] or by potential trans-glutathionylation mechanisms, analogous to previously established thiol-disulfide exchange mechanisms that transmit redox signals [43,44]. Follow-up studies that more directly probe initial thiol oxidation to sulfenic acids (e.g. [45,46]) will be critical to better evaluate such proximal oxidant signals in relation to DUOX1 activation.

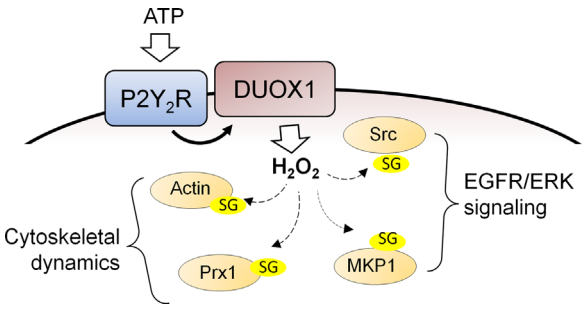

Fig. 5. Schematic illustration of DUOX1-dependent *S*-glutathionylation of target proteins and their roles in ATP-dependent cell migration. Exogenous ATP stimulates purinergic $P2Y_2$ receptors to activate DUOX1-dependent production of H_2O_2, which in turn promotes *S*-glutathionylation (–SG) of several target proteins that play specific roles in ATP-dependent cell signaling and regulation of cytoskeletal dynamics to promote cell spreading and migration.

Acknowledgments

The authors would like to thank Lucia Y. Brown in the Department of Obstetrics, Gynecology, and Reproductive Sciences, for her generous assistance with immunofluorescence imaging. This work was supported by the National Institutes of Health [Grants HL085646, HL079331 and NCRR-COBRE P20 RR15557]. Miklos Geiszt is supported by a "Lendulet" grant from the Hungarian Academy of Sciences. The Proteomics Facility is supported by the Vermont Genetics Network through NIH Grant 8P20GM103449.

Appendix A. Supporting information

Supplementary data associated with this article can be found in the online version at http://dx.doi.org/10.1016/j.redox.2013.12.030.

References

[1] P. Moskwa, D. Lorentzen, K.J. Excoffon, J. Zabner, P.B. McCray , W.M. Nauseef, C. Dupuy, B. Banfi, A novel host defense system of airways is defective in cystic fibrosis, Am. J. Respir. Crit. Care Med. 175 (2007) 174–183.
[2] M. Geiszt, J. Witta, J. Baffi, K. Lekstrom, T.L. Leto, Dual oxidases represent novel hydrogen peroxide sources supporting mucosal surface host defense, FASEB J. 17 (2003) 1502–1504.
[3] E.M. Ha, K.A. Lee, Y.Y. Seo, S.H. Kim, J.H. Lim, B.H. Oh, J. Kim, W.J. Lee, Coordination of multiple dual oxidase-regulatory pathways in responses to commensal and infectious microbes in drosophila gut, Nat. Immunol. 10 (2009) 949–957.
[4] M.V. Flores, K.C. Crawford, L.M. Pullin, C.J. Hall, K.E. Crosier, P.S. Crosier, Dual oxidase in the intestinal epithelium of zebrafish larvae has anti-bacterial properties, Biochem. Biophys. Res. Commun. (2010)164–168.
[5] X.D. Deken, B. Corvilain, J.E. Dumont, F. Miot, Roles of DUOX-mediated hydrogen peroxide in metabolism, host defense, and signaling, Antioxid Redox Signal. (2013) [Epub ahead of print].
[6] M.T. Juarez, R.A. Patterson, E. Sandoval-Guillen, W. McGinnis, Duox, Flotillin-2, and Src42A are required to activate or delimit the spread of the transcriptional response to epidermal wounds in Drosophila, PLoS Genet. 7 (2011) e1002424.
[7] P. Niethammer, C. Grabher, A.T. Look, T.J. Mitchison, A tissue-scale gradient of hydrogen peroxide mediates rapid wound detection in zebrafish, Nature 459 (2009) 996–999.
[8] S.K. Yoo, C.M. Freisinger, D.C. Lebert, A. Huttenlocher, Early redox, Src family kinase, and calcium signaling integrate wound responses and tissue regeneration in zebrafish, J. Cell Biol. 199 (2012) 225–234.
[9] S.H. Gorissen, M. Hristova, A. Habibovic, L.M. Sipsey, P.C. Spiess, Y.M. Janssen-Heininger, A. van der Vliet, Dual oxidase-1 is required for airway epithelial cell migration and bronchiolar reepithelialization after injury, Am. J. Respir. Cell Mol. Biol. 48 (2013) 337–345.
[10] A. van der Vliet, Y.M. Janssen-Heininger, Hydrogen peroxide as a damage signal in tissue injury and inflammation: murderer, mediator, or messenger? J. Cell. Biochem. (2013) [Epub ahead of print].
[11] D. Sham, U.V. Wesley, M. Hristova, A. van der Vliet, ATP-mediated transactivation of the epidermal growth factor receptor in airway epithelial cells involves DUOX1-dependent oxidation of Src and ADAM17, PLoS One 8 (2013) e54391.

[12] U.V. Wesley, P.F. Bove, M. Hristova, S. McCarthy, A. van der Vliet, Airway epithelial cell migration and wound repair by ATP-mediated activation of dual oxidase 1, J. Biol. Chem. 282 (2007) 3213–3220.
[13] J.L. Koff, M.X. Shao, I.F. Ueki, J.A. Nadel, Multiple TLRs activate EGFR via a signaling cascade to produce innate immune responses in airway epithelium, Am. J. Physiol. Lung Cell Mol. Physiol. 294 (2008) L1068–L1075.
[14] A.W. Boots, M. Hristova, D.I. Kasahara, G.R. Haenen, A. Bast, A. van der Vliet, ATP-mediated activation of the NADPH oxidase DUOX1 mediates airway epithelial responses to bacterial stimuli, J. Biol. Chem. 284 (2009) 17858–17867.
[15] L. Wang, H. Zhen, W. Yao, F. Bian, F. Zhou, X. Mao, P. Yao, S. Jin, Lipid raft-dependent activation of dual oxidase 1/H_2O_2/NF-kappaB pathway in bronchial epithelial cells, Am. J. Physiol. Cell Physiol. 301 (2011) C171–C180.
[16] B. Enyedi, M. Zana, A. Donko, M. Geiszt, Spatial and temporal analysis of NADPH oxidase-generated hydrogen peroxide signals by novel fluorescent reporter proteins, Antioxid Redox Signal. 19 (2013) 523–534.
[17] Y.M. Janssen-Heininger, B.T. Mossman, N.H. Heintz, H.J. Forman, B. Kalyanaraman, T. Finkel, J.S. Stamler, S.G. Rhee, A. van der Vliet, Redox-based regulation of signal transduction: principles, pitfalls, and promises, Free Radic. Biol. Med. 45 (2008) 1–17.
[18] Y. Xiong, J.D. Uys, K.D. Tew, D.M. Townsend, S-glutathionylation: from molecular mechanisms to health outcomes, Antioxid Redox Signal. **15** (2011) 233–270.
[19] N.L. Reynaert, K. Ckless, A.S. Guala, E.F. Wouters, A. van der Vliet, Y.M. Janssen-Heininger, In situ detection of S-glutathionylated proteins following glutaredoxin-1 catalyzed cysteine derivatization, Biochim. Biophys. Acta 1760 (2006) 380–387.
[20] A.M. Evangelista, M.D. Thompson, R.M. Weisbrod, D.R. Pimental, X. Tong, V.M. Bolotina, R.A. Cohen, Redox regulation of SERCA2 is required for vascular endothelial growth factor-induced signaling and endothelial cell migration, Antioxid Redox Signal. 17 (2012) 1099–1108.
[21] J. Sakai, J. Li, K.K. Subramanian, S. Mondal, B. Bajrami, H. Hattori, Y. Jia, B.C. Dickinson, J. Zhong, K. Ye, C.J. Chang, Y.S. Ho, J. Zhou, H.R. Luo, Reactive oxygen species-induced actin glutathionylation controls actin dynamics in neutrophils, Immunity 37 (2012) 1037–1049.
[22] H.S. Kim, S.L. Ullevig, D. Zamora, C.F. Lee, R. Asmis, Redox regulation of MAPK phosphatase 1 controls monocyte migration and macrophage recruitment, Proc. Natl. Acad. Sci. USA 109 (2012) E2803–E2812.
[23] M.A. Abdelsaid, A.B. El-Remessy, S-glutathionylation of LMW-PTP regulates VEGF-mediated FAK activation and endothelial cell migration, J. Cell Sci. 125 (2012) 4751–4760.
[24] R. Wu, D. Smith, Continuous multiplication of rabbit tracheal epithelial cells in a defined, hormone-supplemented medium, In Vitro 18 (1982) 800–812.
[25] J.F. Alcorn, A.S. Guala, J. van der Velden, B. McElhinney, C.G. Irvin, R.J. Davis, Y.M. Janssen-Heininger, Jun N-terminal kinase 1 regulates epithelial-to-mesenchymal transition induced by TGF-beta1, J. Cell Sci. 121 (2008) 1036–1045.
[26] A. Donko, E. Ruisanchez, A. Orient, B. Enyedi, R. Kapui, Z. Peterfi, X. de Deken, Z. Benyo, M. Geiszt, Urothelial cells produce hydrogen peroxide through the activation of Duox1, Free Radic. Biol. Med. 49 (2010) 2040–2048.
[27] R. Priora, L. Coppo, S. Salzano, P. Di Simplicio, P. Ghezzi, Measurement of mixed disulfides including glutathionylated proteins, Methods Enzymol. 473 (2010) 149–159.
[28] A. van der Vliet, C.A. O'Neill, C.E. Cross, J.M. Koostra, W.G. Volz, B. Halliwell, S. Louie, Determination of low-molecular-mass antioxidant concentrations in human respiratory tract lining fluids, Am. J. Physiol. 276 (1999) L289–L296.
[29] D.M. Sullivan, N.B. Wehr, M.M. Fergusson, R.L. Levine, T. Finkel, Identification of oxidant-sensitive proteins: TNF-alpha induces protein glutathiolation, Biochemistry 39 (2000) 11121–11128.
[30] D.P. Jones, J.L. Carlson, P.S. Samiec, P. Sternberg , V.C. Mody , R.L. Reed, L.A. Brown, Glutathione measurement in human plasma. Evaluation of sample collection, storage and derivatization conditions for analysis of dansyl derivatives by HPLC, Clin. Chim. Acta 275 (1998) 175–184.
[31] J.V. Cordeiro, A. Jacinto, The role of transcription-independent damage signals in the initiation of epithelial wound healing, Nat. Rev. Mol. Cell Biol. 14 (2013) 249–262.
[32] A. van der Vliet, NADPH oxidases in lung biology and pathology: host defense enzymes, and more, Free Radic. Biol. Med. 44 (2008) 938–955.
[33] A. Daiber, Redox signaling (cross-talk) from and to mitochondria involves mitochondrial pores and reactive oxygen species, Biochim. Biophys. Acta 1797 (2010) 897–906.
[34] S. Dikalov, Cross talk between mitochondria and NADPH oxidases, Free Radic. Biol. Med. 51 (2011) 1289–1301.
[35] T.J. Myers, L.H. Brennaman, M. Stevenson, S. Higashiyama, W.E. Russell, D.C. Lee, S.W. Sunnarborg, Mitochondrial reactive oxygen species mediate GPCR-induced TACE/ADAM17-dependent transforming growth factor-alpha shedding, Mol. Biol. Cell 20 (2009) 5236–5249.
[36] R.H. Insall, L.M. Machesky, Actin dynamics at the leading edge: from simple machinery to complex networks, Dev. Cell 17 (2009) 310–322.
[37] J. Wang, E.S. Boja, W. Tan, E. Tekle, H.M. Fales, S. English, J.J. Mieyal, P.B. Chock, Reversible glutathionylation regulates actin polymerization in A431 cells, J. Biol. Chem. 276 (2001) 47763–47766.
[38] T. Fiaschi, G. Cozzi, G. Raugei, L. Formigli, G. Ramponi, P. Chiarugi, Redox regulation of beta-actin during integrin-mediated cell adhesion, J. Biol. Chem. 281 (2006) 22983–22991.
[39] J.W. Park, G. Piszczek, S.G. Rhee, P.B. Chock, Glutathionylation of peroxiredoxin I induces decamer to dimers dissociation with concomitant loss of chaperone activity, Biochemistry 50 (2011) 3204–3210.
[40] H.Z. Chae, H. Oubrahim, J.W. Park, S.G. Rhee, P.B. Chock, Protein glutathionylation in the regulation of peroxiredoxins: a family of thiol-specific peroxidases that function as antioxidants, molecular chaperones, and signal modulators, Antioxid Redox Signal. 16 (2012) 506–523.
[41] H.A. Woo, S.H. Yim, D.H. Shin, D. Kang, D.Y. Yu, S.G. Rhee, Inactivation of peroxiredoxin I by phosphorylation allows localized $H(_2)O(_2)$ accumulation for cell signaling, Cell 140 (2010) 517–528.
[42] B. Turner-Ivey, Y. Manevich, J. Schulte, E. Kistner-Griffin, A. Jezierska-Drutel, Y. Liu, C.A. Neumann, Role for Prdx1 as a specific sensor in redox-regulated senescence in breast cancer, Oncogene 32 (2013) 5302–5314.
[43] S.G. Rhee, H.A. Woo, I.S. Kil, S.H. Bae, Peroxiredoxin functions as a peroxidase and a regulator and sensor of local peroxides, J. Biol. Chem. 287 (2012) 4403–4410.
[44] D.E. Fomenko, A. Koc, N. Agisheva, M. Jacobsen, A. Kaya, M. Malinouski, J.C. Rutherford, K.L. Siu, D.Y. Jin, D.R. Winge, V.N. Gladyshev, Thiol peroxidases mediate specific genome-wide regulation of gene expression in response to hydrogen peroxide, Proc. Natl. Acad. Sci. USA 108 (2011) 2729–2734.
[45] C.E. Paulsen, T.H. Truong, F.J. Garcia, A. Homann, V. Gupta, S.E. Leonard, K.S. Carroll, Peroxide-dependent sulfenylation of the EGFR catalytic site enhances kinase activity, Nat. Chem. Biol. 8 (2012) 57–64.
[46] K.J. Nelson, C. Klomsiri, S.G. Codreanu, L. Soito, D.C. Liebler, L.C. Rogers, L.W. Daniel, L.B. Poole, Use of dimedone-based chemical probes for sulfenic acid detection methods to visualize and identify labeled proteins, Methods Enzymol. 473 (2010) 95–115.